The Hydrogen Binding Site in Hydrogenase: 35-GHz ENDOR and XAS Studies of the Ni-C Active Form and the Ni-L Photoproduct

Joyce P. Whitehead,[†] Ryszard J. Gurbiel,[‡,§] Csaba Bagyinka,[†,∥] Brian M. Hoffman,*[,‡] and Michael J. Maroney*[,†,⊥]

Contribution from the Department of Chemistry and the Program in Molecular and Cellular Biology, University of Massachusetts, Amherst, Massachusetts 01003, and the Department of Chemistry, Northwestern University, Evanston, Illinois 60208

Received July 30, 1992

Abstract: EPR, 35-GHz ENDOR, and X-ray absorption (XAS) spectroscopic studies of H_2 binding in hydrogenase from *Thiocapsa roseopersicina* are reported. These studies involve spectra taken on an active form of the enzyme that displays an EPR signal designated Ni-C. This form of the enzyme is light sensitive and is converted to a photoproduct that exhibits a unique EPR signal, Ni-L. ^{1}H-ENDOR spectra reveal two sets of protons that interact strongly with the EPR-active center in Ni-C. The first proton set (H1) is solvent exchangeable, originates from dihydrogen, and has a value of A(H1) $\sim$ 20 MHz. The second proton set (H2) is not solvent exchangeable, has a coupling constant of A(H2) $\sim$ 12 MHz, and is assigned to one or more cysteine β-CH_2 protons. Upon irradiation and conversion of the EPR signal to Ni-L, the exchangeable H1 proton set is no longer observed. Upon annealing and regeneration of Ni-C, the feature associated with the H1 proton set is again observed. This is direct evidence that the photoprocess and annealing involve dissociation of a hydrogenic proton and recombination. XAS spectra taken on samples poised to maximize Ni-C and Ni-L do not reveal any significant structural difference between the Ni sites.

Hydrogenases (H_2ases) are metalloenzymes that catalyze the reversible two-electron oxidation of dihydrogen.[1-3] This diverse group of enzymes is found in a wide variety of prokaryotes and eukaryotes, and they have been classified according to the inorganic cofactors present.[4-6] The majority of H_2ases contain Fe,S clusters and a Ni center that is believed to be a component of the H_2-activating site (Fe,Ni H_2ases). The presence of Ni in the enzyme is usually revealed by the observation of one or more EPR signals that have been attributed to $S = {}^1/_2$ Ni sites using ^{61}Ni-labeled enzymes.[7,8] Distinct EPR signals are observed for two oxidized and catalytically inactive forms of the enzyme (Ni-A and Ni-B), as well as for a reduced and active form (Ni-C) of the enzyme. Typically, when Fe,Ni H_2ases are isolated aerobically, they are isolated in the oxidized forms that can be activated under reducing conditions.[7,9] Under H_2 atmosphere, the signals associated with the oxidized forms disappear, yielding an EPR silent intermediate. Further exposure to H_2 causes the appearance of the signal (Ni-C) that is associated with the active form of the enzyme. A fully reduced form of the enzyme that is also EPR silent is produced under extensive incubation with H_2.

The active form of the enzyme is characterized by a rhombic EPR signal, Ni-C, that has been attributed to a Ni complex of H^- or H_2 based on EPR and ENDOR spectroscopic studies.[10-12] The active enzyme is light sensitive and is known to be converted to a photoproduct by exposure to visible light at low temperature.[9,10,13] The photoproduct exhibits a distinct EPR signal, Ni-L. The photochemistry is reversible; annealing the sample at a higher temperature regenerates the Ni-C EPR spectrum. We report the results of EPR, 35-GHz ENDOR, and X-ray absorption spectroscopic (XAS) studies of the active form of *Thiocapsa roseopersicina* H_2ase and its photoproduct. ENDOR offers a direct probe of the protons and deuterons derived from H_2 and D_2O that are bound in the enzyme. These studies provide the first direct evidence that the processes involved are photodissociation and recombination of H^+, H^- or H_2. Analysis of the Ni K-edge XAS spectra reveals that no significant change in the oxidation state of Ni, the geometry of the Ni site, the endogenous ligand environment of the Ni center, or the Ni–ligand bond lengths occurs in the photoprocess.

Results

EPR. The EPR signal of the active form of *Thiocapsa roseopersicina* (Ni-C) is characterized by the g-tensor $g^{C}_{1,2,3}$ = 2.19, 2.15, and 2.02 (Figure 1). The principal g-values of the photoproduct produced by illuminating the active enzyme with visible light (Ni-L) are $g^{L}_{1,2,3}$ = 2.29, 2.13, and 2.05 (Figure 1). These values are in agreement with previously published values[13] and are similar to those observed in a number of Fe,Ni H_2ases

† Department of Chemistry, University of Massachusetts.
‡ Department of Chemistry, Northwestern University.
§ On leave from the Institute of Molecular Biology, Jangiellonian University, Krakow, Poland.
∥ Current address: Institute of Biophysics, Biological Research Center of the Hungarian Academy of Sciences, H-6701, Szeged, Hungary.
⊥ Program in Molecular and Cellular Biology.

(1) Adams, M. W. W. *Biochim. Biophys. Acta* **1990**, *1020*, 115–45.
(2) Przybyla, A. E.; Robbins, J.; Menon, N.; Peck, H. D. J. *FEMS Microbiol. Rev.* **1992**, *88*, 109–35.
(3) Cammack, R.; Hall, D. O.; Rao, K. K. In *Microbial Gas Metabolism*; Poole, K. K., Dow, C., Eds.; Academic Press: London, 1985; Chapter 4.
(4) Lorenz, B.; Schneider, K.; Kratzin, H.; Schlegel, H. G. *Biochim. Biophys. Acta* **1989**, *995*, 1–9.
(5) Kovacs, K. L.; Seefeldt, L. C.; Tigyi, G.; Doyle, C. M.; Mortenson, L. E.; Arp, D. J. *J. Bacteriol.* **1989**, *171*, 430–5.
(6) Fauque, G.; Teixeira, M.; Moura, I.; Lespinat, P. A.; Xavier, A. V.; Der, V. D.; Peck, H. J.; Le, G. J.; Moura, J. G. *Eur. J. Biochem.* **1984**, *142*, 21–8.
(7) Moura, J. J. G.; Teixeira, M.; Moura, I.; LeGall, J. In *The Bioinorganic Chemistry of Nickel*; Lancaster, J. R., Jr.; Ed.; VCH: New York, 1988; pp 191–226.
(8) Moura, J. J. G.; Teixeira, M.; Xavier, A. V.; Moura, I.; LeGall, J. *J. Mol. Catal.* **1984**, *23*, 303.
(9) Cammack, R.; Fernandez, V. M.; Schneider, K. In *The Bioinorganic Chemistry of Nickel*; Lancaster, J. R., Ed.; VCH: New York, 1988; Chapter 8.
(10) van der Zwaan, J. W.; Albracht, S. P.; Fontijn, R. D.; Slater, E. C. *FEBS Lett.* **1985**, *179*, 271–7.
(11) van der Zwaan, J. W.; Coremans, J. M. C. C.; Bouwens, E. C. M.; Albracht, S. P. J. *Biochim. Biophys. Acta* **1990**, *1041*, 101–10.
(12) Fan, C.; Teixeira, M.; Moura, J.; Moura, I.; Huynh, B. H.; Le, G. J.; Peck, H. D. J.; Hoffman, B. M. *J. Am. Chem. Soc.* **1991**, *113*, 20–4.
(13) Cammack, R.; Bagyinka, C.; Kovacs, K. L. *Eur. J. Biochem.* **1989**, *182*, 357–62.

0002-7863/93/1515-5629$04.00/0 © 1993 American Chemical Society

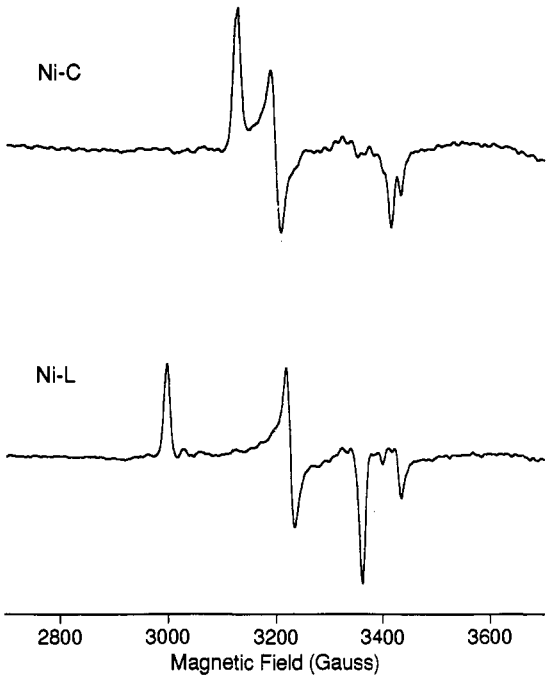

Figure 1. EPR spectra of *Thiocapsa roseopersicina* hydrogenase, Ni-C and Ni-L. Spectra were taken at 77 K, at a microwave frequency of 9.62 GHz, a microwave power of 20 mW, and a modulation amplitude of 4 G.

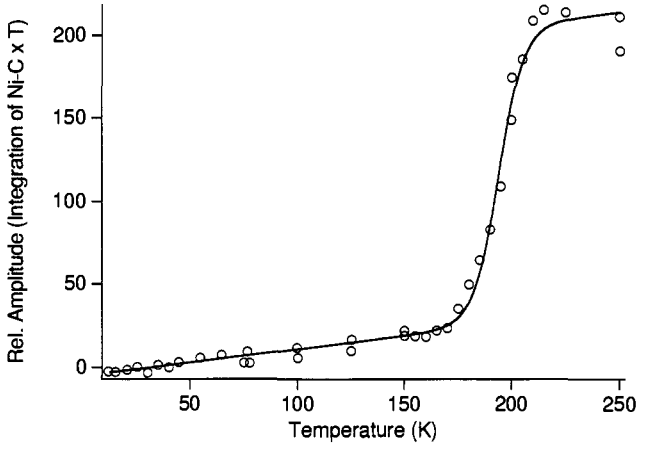

Figure 2. The temperature dependence of the annealing process shown as the integration of the Ni-C signal (multiplied by the temperature) arising from annealing of a sample originally exhibiting only the Ni-L signal (o data points; —, fit = exponential jump function).

from a variety of sources.[7,9] A significant advantage to the use of the *Thiocapsa* enzyme in the ENDOR studies of Ni-C and Ni-L described below is that their EPR spectra at low temperature do not overlap signals from Fe,S clusters. Thus, ENDOR spectra can be taken at multiple fields. In contrast, ENDOR spectra of *D. gigas* H_2ase Ni-C could only be taken near g_1.[12]

It has been reported that the photochemical process involved in the conversion of Ni-C to Ni-L is reversed by annealing the sample near 200 K.[10,13] Our results confirm the reversibility of the photoprocess for at least three cycles of annealing. The transition temperature for the annealing process was determined to be 194 K by monitoring the sample composition at different temperatures (Figure 2).

35-GHz ENDOR. Samples of enzyme poised to maximize the Ni-C EPR signal were prepared by adjusting the H_2 concentration over the sample in the absence of redox mediators. After the ENDOR spectra of Ni-C were collected, the samples were converted to Ni-L by exposure to light. The EPR spectra of Ni-C and Ni-L are distinct, but they overlap for $g_{obs} \leq 2.19$. However, even if photoconversion is incomplete, Ni-L can be observed alone for $2.29 \leq g_{obs} \leq 2.19$. Annealed samples of Ni-L regenerated both the EPR and ENDOR spectrum of Ni-C.

A ^{1}H-ENDOR spectrum of the Ni-C center in H_2O taken at g_2 (Figure 3A) shows a pattern distorted by relaxation effects, with both positive and negative features. Positive features include the sharp peak at $\delta\nu_H = \nu - \nu_H \approx -6$ MHz and a much broader peak at $\delta\nu_H \approx +10$ MHz; negative ones include an intense peak at $\delta\nu_H = +6$ MHz and a much weaker and broader feature at $\delta\nu_H \approx -10$ MHz. By matching features into ν_+, ν_- pairs according to eq 1, hyperfine-split doublets with $A(^1H1) \approx 20$ MHz and $A(^1H2) \approx 12$ MHz can be assigned, along with additional intensity with $A < 5$ MHz. Similar relaxation effects are seen in a ^{1}H spectrum taken at g_1 (Figure 4A). However, the ν_+ features of H1 and H2 are clearly distinguished here. Comparison of the spectra at g_1 and g_2 shows that the H2 coupling is isotropic, $A(^1H2) \approx 12$ MHz, but that $A(^1H1)$ is somewhat smaller at g_1, $A(^1H1) \approx 16$–18 MHz.

The ^{2}H-ENDOR spectrum at g_2 for the Ni-C sample prepared in D_2O (Figure 3C) shows a hyperfine-split doublet with $A(^2H1) \approx 3.1$ MHz that corresponds to the H1 proton coupling ($A(^1H1) \approx 21.5$ MHz). Thus the H1 protons are exchangeable upon deuteration of the solvent. In contrast, there is no ^{2}H signal that corresponds to the 12-MHz ^{1}H coupling, showing that the H2 set is nonexchangeable. The g_2 and g_1 ^{1}H-ENDOR spectra of the sample in D_2O are presented in Figures 3B and 4B, respectively. This sample has a much lower concentration of Ni-C centers and thus the ENDOR pattern is noisier than that of the sample in H_2O (Figure 3A). As expected from the ^{2}H data, the ^{1}H1 doublet is greatly diminished by H/D exchange, as seen most clearly at g_1 (Figure 4). Nevertheless, the spectra taken at g_1 and g_2 still show broad features at $\delta\nu = +10$ MHz and weak residual intensity at ± 8 MHz, respectively, which likely persist because H/D exchange is not complete for H1. Again, as anticipated from the ^{2}H data, the feature observed in the g_2 ^{1}H-ENDOR spectrum of Ni-C in H_2O at $\delta\nu \approx -6$ MHz ($A(H2) \sim 12$ MHz) remains present in the ^{1}H-ENDOR spectra of Ni-C in D_2O. The ^{1}H spectrum in D_2O taken at g_1 (Figure 4B) shows this even more clearly; both peaks of the nonexchangeable H1 doublet now are of comparable intensity. The spectrum confirms that $A(^1H2) \approx 12$ MHz and is isotropic.

These results are very similar to those previously reported for *D. gigas* hydrogenase. There, two classes of exchangeable protons were reported, with hyperfine coupling of 17 and 4 MHz, respectively, along with a class of nonexchangeable proton with hyperfine coupling of 12 MHz.[12] The exchangeable H1 proton doublet with $A(H1) \approx 20$ MHz seen here is assigned to a proton(s) derived from H_2 in analogy with the previous study. The more weakly coupled exchangeable proton(s) seen before is not detectable in the present study. One possible reason for this is the presence of a strong and broad feature centered at proton and deuteron Larmor frequencies that could be obscuring the peaks from weakly coupled exchangeable protonic species.

Irradiation of Ni-C converts it to Ni-L. Figure 3D shows the ^{1}H-ENDOR spectrum obtained at g_2 from Ni-L in H_2O. Comparison of this spectrum for Ni-L with a corresponding spectrum for Ni-C (Figure 3A) shows that the features at $\delta\nu = \pm 10$ MHz are almost completely lost upon photolysis. Likewise, the ^{2}H-ENDOR spectrum of Ni-L in H_2O shows no features from H1 deuterons (Figure 3F), unlike the ^{2}H-ENDOR spectrum of Ni-C in D_2O (Figure 3C). *These results indicate that formation of Ni-L by photolysis involves dissociation of the H1 protons from the EPR active center.* The ^{1}H-ENDOR spectra of the Ni-L sample in D_2O at g_2 (Figure 3E) and at g_1 have lost all residual intensity at $\delta\nu = \pm 10$ MHz. This result is expected if the remaining intensity at $\sim \pm 10$ MHz in Figure 3D is associated with incomplete photolysis of exchangeable H1 protons. In

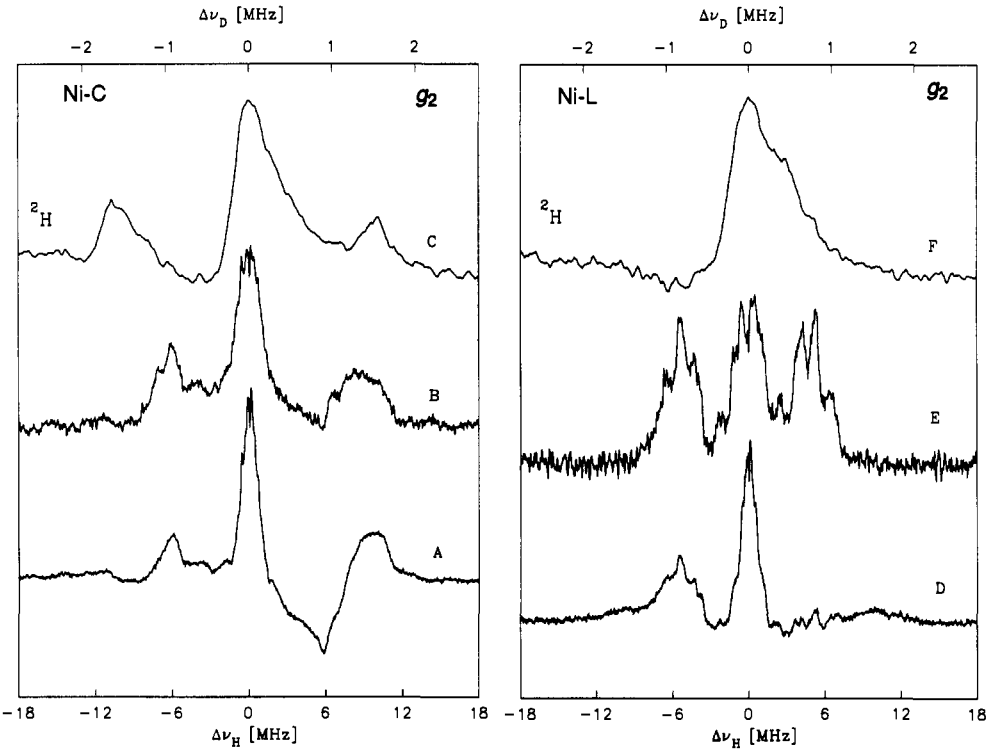

Figure 3. 35-GHz ^{1}H- and ^{2}H-ENDOR spectra of Ni-C and Ni-L taken at g_2: (A) ^{1}H-ENDOR spectrum of Ni-C in H_2O; (B) ^{1}H-ENDOR spectrum of Ni-C in D_2O; (C) ^{2}H-ENDOR spectrum of Ni-C in D_2O; (D) ^{1}H-ENDOR spectrum of Ni-L in H_2O; (E) ^{1}H-ENDOR spectrum of Ni-L in D_2O; (F) ^{2}H-ENDOR spectrum of Ni-L in D_2O. The upper axis gives frequencies of ^{2}H resonances on the scale adjusted according to eq 2. Parameters: microwave power = 0.32 mW, RF power = 35 W, time constant = 32 ms, modulation amplitude = 0.4 (protons) or 0.8 G (deuterons), scan rate = 0.4 (protons) or 0.8 MHz/s (deuterons).

Table I. Comparison of Ni-C and Ni-L Samples Used in XAS Experiments

enzyme sample	Ni K-edge energy ±0.2 (eV)	1s → 3d peak area ±0.005 eV (rel to $NiCl_4^{2-}$)[14]	S/N	% of Ni EPR detectable[a]	% of EPR active Ni poised[b]
C	8339.5	<0.001 (<0.01)	600	71	100
L	8339.4	0.012 (0.140)	460	65	100

[a] Based on protein concentration determination and 1.0 Ni/protein.[15] [b] Percentage of EPR active Ni poised in the desired form. A value of 100% indicates a single EPR active species is present.

contrast to the H1 proton set, the H2 proton set is neither photolabile nor exchangeable. Thus, the $\delta\nu_-(^1H2) \approx -6$ MHz feature is seen in the g_2 spectrum of Ni-L in H_2O (Figure 3D), and both $\delta\nu_\pm(^1H2)$ peaks are seen in the g_2 (Figure 3E) and g_1 (Figure 4B) spectra of Ni-L in D_2O. However, the coupling to H2 is slightly smaller in Ni-L than in Ni-C, and it has become mildly anisotropic. Thus, for Ni-L $A(^1H2) \approx 10$ MHz at g_2 (Figure 3E) and ≈8 MHz at g_1 (Figure 4C), as compared to the isotropic $A(^1H2) \approx 12$ MHz for Ni-C. Further, the H2 pattern of Ni-L in D_2O at g_2 clearly shows resolved structure (Figure 3E) that is only indicated (barely) in the ν_- peak of Ni-C (Figure 3B). In principle, such structure could arise from the presence of several slightly inequivalent H2 protons, from the effects of hyperfine anisotropy, or from some combination of the two. The observation of sharp lines in the single-crystal-like spectra of Ni-C and Ni-L at g_1 (Figure 4, B and C, respectively) perhaps favors a single proton and certainly indicates that any inequivalence among multiple H2 protons is likely to arise not from chemical differences but rather from differently oriented hyperfine tensors. However, given the low levels of anisotropy that are associated with the H2 protons, it is not impossible that H2 represents more than one proton.

XAS. Ni K-edge XANES spectra for a Ni-C sample and its photoproduct following illumination with visible light are compared in Figure 5 and Table I. No significant difference between the spectra before and after illumination can be discerned. The nearly featureless edges and low 1s-3d peak areas are consistent with six-coordinate or possibly five-coordinate trigonal-bipyramidal Ni sites in both cases.[14] The similarity of the two spectra in the XANES region indicates that the geometry and the endogenous ligand environment of the Ni center are unchanged upon photolysis. The edge energy of both samples is constant within the precision of the experiment (±0.2 eV), indicating that the electron density residing on the Ni center is not perturbed by the photolysis.

The lack of change in the Ni ligand environment is confirmed by analysis of the Ni K-edge EXAFS spectra. Figures 6 and 7 illustrate the analyses of Fourier-filtered and unfiltered EXAFS data, respectively. The best fits using Fourier-filtered and unfiltered data determined by minimizing both R and σ^2 are summarized in Table II. A complete set of fits from one, two, and three shell fits using the restricted fit protocol[16] is available as supplementary material. The Ni-C and Ni-L EXAFS spectra are indistinguishable. Both samples are best fit by a model that contains three shells of scattering atoms: 1 or 2 N(O) at 1.93(2) Å, 3 ± 1 S(Cl) at 2.23(2) Å, and 1 S(Cl) at 2.73(3) Å. There is no significant difference between fits generated by using Fourier-filtered or unfiltered data.

(14) Colpas, G. J.; Maroney, M. J.; Bagyinka, C.; Kumar, M.; Willis, W. S.; Suib, S. L.; Mascharak, P. K.; Baidya, N. *Inorg. Chem.* **1991**, *30*, 920–8.
(15) Bagyinka, C.; Whitehead, J. P.; Maroney, M. J. *J. Am. Chem. Soc.*, submitted for publication.
(16) Scarrow, R. C.; Maroney, M. J.; Palmer, S. M.; Que, L., Jr.; Roe, A. L.; Salowe, S. P.; Stubbe, J. *J. Am. Chem. Soc.* **1987**, *109*, 7857–64.

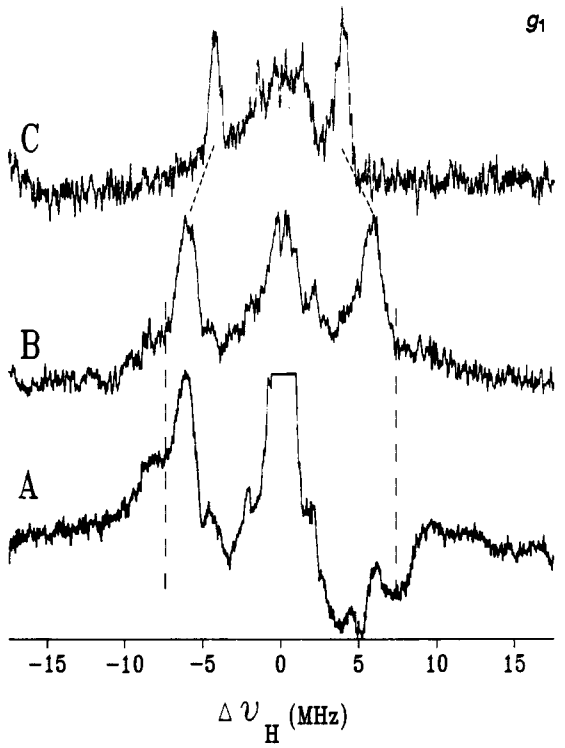

Figure 4. Comparison of the 35-GHz ^{1}H-ENDOR spectra taken at g_1: (A) Ni-C in H_2O and (B) in D_2O; (C) Ni-L taken in D_2O. The dashed lines illustrate the loss of intensity for ^{1}H(1) for Ni-C in D_2O (B). The dotted line illustrates the difference in $A(^1H2)$ between Ni-C (B) and Ni-L (C). Conditions as in Figure 3. In spectrum C, the intense distant ENDOR peak from solvent H_2O has been suppressed.

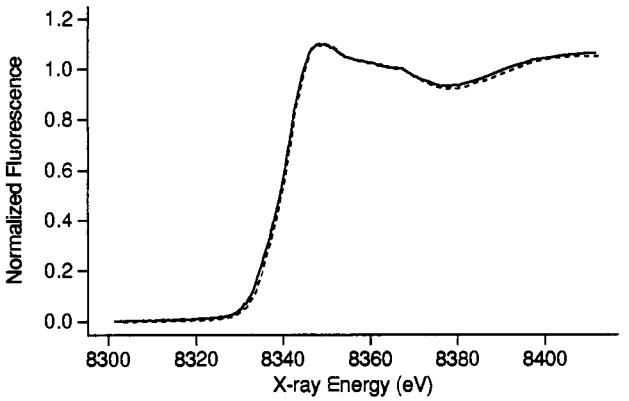

Figure 5. Ni K-edge XANES spectra of C (—) and L (- - -) samples of *Thiocapsa roseopersicina* hydrogenase.

Discussion

The light sensitivity of Ni-C has been observed for H_2ases from a variety of sources including *Thiocapsa roseopersicina*,[13] *Desulfovibrio gigas*,[17] *and Chromatium vinosum*,[10] and therefore it appears to be a general property of this active form of the enzyme. The association of Ni-C with the formation of a Ni hydride or dihydrogen complex has been made on the basis of EPR and ENDOR studies.[11,12] Previous EPR studies have demonstrated that the photochemical process is reversible upon annealing at temperatures above liquid N_2 temperature (e.g. 200 K).[10] Since the photochemical process was accompanied by a change in the EPR signal attributed to the Ni center, it was suggested that it involved a change in the Ni ligand environment.[10]

The 35-GHz ENDOR spectroscopic investigations of active H_2ase from *T. roseopersicina* clearly show resolved resonances from two distinct types of protons coordinated to the center giving rise to the Ni-C EPR signal: strongly coupled (A(H1) ≈ 20 MHz) exchangeable protons and more weakly coupled (A(H2)

(17) Cammack, R.; Patil, V. S.; Fernandez, V. M. *Biochim. Biophys. Acta* **1985**, *912*, 98–109.

Table II. Analysis of Ni K-Edge EXAFS Data for Ni-C and Ni-L

no. of shells	N	r (Å)	$10^3\Delta\sigma^2$ (Å^2)	correlations >0.6	R
		C, filtered data			
1	4	Ni–S = 2.218(1)	4.8		0.47
2	1	Ni–N = 1.917(15)	4.8		**0.48**
	3	Ni–S = 2.222(2)	2.3		
	3	Ni–S = 2.219(1)	1.1		0.32
	1	Ni–S = 2.750(4)	1.8		
3	1	Ni–N = 1.924(4)	5.6		**0.12**
	3	Ni–S = 2.222(1)	2.5		
	1	Ni–S = 2.748(2)	2.7		
	2	Ni–N = 1.960(4)	5.6		0.26
	2	Ni–S = 2.227(1)	–0.2		
	1	Ni–S = 2.743(3)	1.7		
	1	Ni–N = 1.956(3)	–3.9	σ_N/σ_{S1}=0.71	0.27
	2	Ni–S = 2.227(1)	–0.8		
	1	Ni–S = 2.744(3)	1.2		
		C, unfiltered data			
1	4	Ni–S = 2.219(2)	5.1		1.11
2	1	Ni–N = 2.000(*a*)	0.0		**1.16**
	3	Ni–S = 2.222(3)	3.2		
	4	Ni–S = 2.218(2)	5.3		1.00
	1	Ni–S = 2.746(10)	3.2		
3	1	Ni–N = 1.917(22)	9.6		**0.99**
	3	Ni–S = 2.221(3)	2.6		
	1	Ni–S = 2.749(8)	1.9		
	2	Ni–N = 1.949(11)	6.9		1.03
	2	Ni–S = 2.224(3)	–0.1		
	1	Ni–S = 2.746(8)	1.3		
	1	Ni–N = 1.947(9)	–3.0		1.02
	2	Ni–S = 2.225(2)	–0.7		
	1	Ni–S = 2.746(8)	1.1		
		L, filtered data			
1	4	Ni–S = 2.219(2)	5.0		0.71
2	1	Ni–N = 1.919(23)	4.6		**0.74**
	4	Ni–S = 2.224(3)	4.9		
	4	Ni–S = 2.221(1)	5.2		0.29
	1	Ni–S = 2.686(3)	0.6		
3	1	Ni–N = 1.935(3)	–4.0	σ_N/σ_{S1}=0.61	**0.27**
	3	Ni–S = 2.228(1)	1.8		
	1	Ni–S = 2.695(2)	–0.3		
	2	Ni–N = 1.959(3)	–2.3	σ_N/σ_{S1}=0.68	0.40
	2	Ni–S = 2.235(1)	–1.1		
	1	Ni–S = 2.697(3)	–1.5		
	1	Ni–N = 1.950(3)	–7.5	σ_N/σ_{S1}=0.77	0.36
	2	Ni–S = 2.231(1)	–1.8		
	1	Ni–S = 2.701(3)	–2.2		
		L, unfiltered data			
1	4	Ni–S = 2.218(2)	4.7		1.21
2	2	Ni–N = 1.942(15)	8.6		**1.30**
	2	Ni–S = 2.224(3)	–0.4		
	4	Ni–S = 2.217(2)	5.2		1.01
	1	Ni–S = 2.694(7)	0.7		
3	1	Ni–N = 1.915(9)	–2.3		**1.01**
	3	Ni–S = 2.224(2)	2.0		
	1	Ni–S = 2.702(6)	–0.9		
	2	Ni–N = 1.945(7)	0.7		1.06
	2	Ni–S = 2.229(2)	–0.7		
	1	Ni–S = 2.702(5)	–1.6		
	1	Ni–N = 1.939(6)	–6.1		1.02
	2	Ni–S = 2.226(2)	–1.4		
	1	Ni–S = 2.701(5)	–2.2		

[a] Not refined.

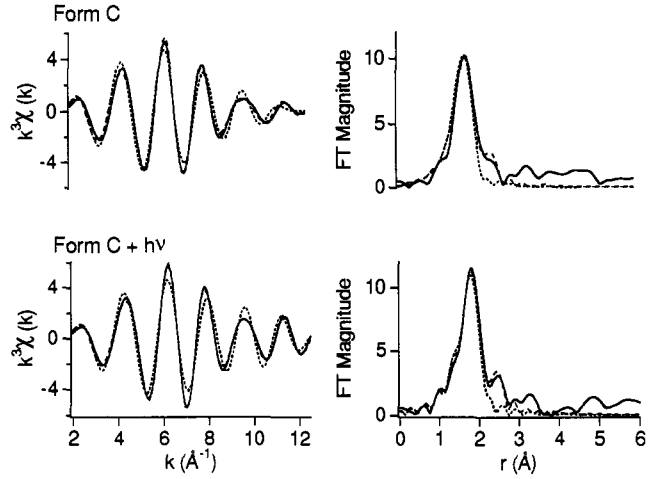

Figure 6. Fourier-transformed and Fourier-filtered EXAFS spectra of the C (—) and L (—) samples of *Thiocapsa roseopersicina* hydrogenase and two (- - -) and three shell (– –) fits from Table II (bold face type). (Transformed spectra are not corrected for phase shift; filtered spectra were generated with a backtransform window of 1.1–2.7 Å).

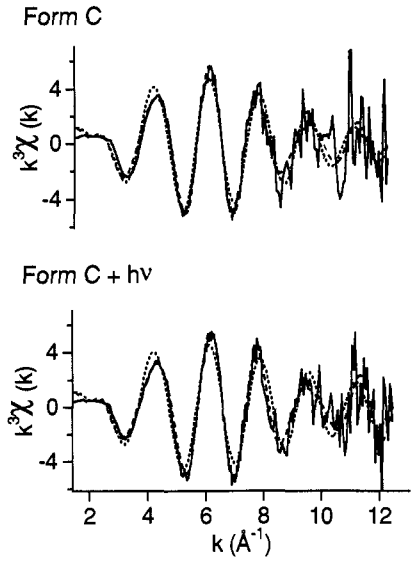

Figure 7. Unfiltered EXAFS spectra of the C (—) and L (—) samples of *Thiocapsa roseopersicina* hydrogenase and two (- - -) and three shell (– –) fits from Table II (bold face type).

≈ 10 MHz) protons that do not exchange upon deuterating the solvent. These results are very similar to those previously reported for *D. gigas* hydrogenase, where two classes of exchangeable protons were reported, with hyperfine coupling of 17 and 4 MHz, respectively, along with a class of nonexchangeable proton with hyperfine coupling of 12 MHz.[12] The exchangeable H1 protons seen in both enzymes are assigned to protons derived from H_2. A more weakly coupled exchangeable proton seen in the *D. gigas* spectrum is not detected in the present study.

The most plausible assignment of the nonexchangeable H2 signal is to cysteine β-CH_2 protons, on the basis of the similarity of these features to those observed in a model compound[18,19] and in other metalloproteins featuring cysteine ligands[22] (histidines would give $A^H < 5$ MHz). The coupling observed is roughly isotropic (A(H2) ≈ 8–12 MHz) and is similar to that observed for nonexchangeable protons in the ENDOR spectra of *D. gigas* H_2ase for Ni-A, Ni-B, and Ni-C;[12] a similar assignment is also appropriate in this case.

The observation of signals attributable to cysteine β-CH_2 protons, coupled with observations of two (or more) S-donor ligands in EXAFS spectra from several H_2ases,[15,20,21] indicates that a substantial amount of spin density resides on Ni-cysteine thiolate ligands in H_2ase. Although it is possible to estimate the spin density on S from the coupling to cysteine β-CH_2 protons,[22-24] the observation of only one coupling permits several possible values. First, the two methylene protons from a single cysteine could have similar and unresolved couplings (A(H2a) ≈ A(H2b) ≈ 10 MHz). Alternatively, the two methylene protons of a cysteinate ligand could have very different couplings, with one coupling too small to resolve (e.g. A(H2a) ≈ 10 MHz and A(H2b) ≤ 2 MHz). Assuming equations presented earlier to be applicable,[22-24] both assignments correspond to a spin density on S, $\sigma_S \approx 0.13$ per sulfur donor atom: the two alternatives differ in the assumed dihedral angle between the S–C–H plane and the Ni–S–C plane ($\theta = \pi/2$ and $\theta = \pi/6$, respectively). If two equivalent cysteines were to contribute to the delocaliation of spin density, the total spin density on S would be ca. 0.26. In this regard, it is noteworthy that the couplings observed for the H_2ase Ni site are similar to those observed for the Cu_A center in cytochrome oxidase, where delocalization over two cysteines is likely.[25]

The ENDOR spectra of the photoinduced Ni-L signal reveal two kinds of changes induced by exposure to light. The most dramatic is that the lines associated with strongly coupled exchangeable protons, H1, are eliminated by light in both ^1H and ^2H spectra. These features have been assigned to a hydrogenic species arising from the binding of the atoms of H_2.[12] Their absence in the illuminated samples and their reappearance in annealed samples indicates that the process involves photodissociation of the hydrogenic species from the paramagnetic center and recombination upon annealing. The possibilities include the photodissociation of a hydride, a proton, or H_2 from the enzyme active site. Homolytic cleavage of a M–H bond is ruled out by the EPR spectrum, which shows no evidence of the production of hydrogen atoms.

The photochemical process also involves a decrease in the coupling of the nonexchangeable H2 protons from 12 MHz in Ni-C to ~8–10 MHz in the photoproduct, which suggests a conformational change within the complex. The decrease in the value of A(H2) in Ni-L indicates a decrease in the total S spin density in the photoproduct and/or a change in dihedral angle.

In contrast to the dramatic change in the EPR and ENDOR spectra of Ni-C upon exposure to light, no change can be discerned in the ligand environment, metal–ligand bond lengths, or Ni oxidation state based on an analysis of the XAS spectra of samples exhibiting only Ni-C and Ni-L EPR signals. The only exception is the change in the 1s → 3d peak area, which increases in the photoproduct and is the correct direction (but not of sufficient magnitude) to be consistent with a change in geometry from six-coordinate to five-coordinate upon photolysis.[14] The analysis of the Ni K-edge EXAFS spectra of Ni-C and Ni-L is not expected to provide evidence for the presence or absence of a H-donor ligand because of the low backscattering cross section of H. However, XAS should reveal changes in the Ni site associated with a change in geometry, oxidation state, spin state, or structure that might be associated with binding and dissociation of a H^- or H_2 ligand. There is no evidence from the XAS analysis to support any such change.

(18) Kumar, M.; Day, R. O.; Colpas, G. J.; Maroney, M. J. *J. Am. Chem. Soc.* **1989**, *111*, 5974–6.
(19) Pressler, M. P.; Gurbiel, R. J.; Hoffman, B. M.; Colpas, G. J.; Kumar, M.; Maroney, M. J. Unpublished results.
(20) Whitehead, J. P.; Colpas, G. J.; Bagyinka, C.; Maroney, M. J. *J. Am. Chem. Soc.* **1991**, *113*, 6288–9.
(21) Maroney, M. J.; Colpas, G. J.; Bagyinka, C.; Baidya, N.; Mascharak, P. K. *J. Am. Chem. Soc.* **1991**, *113*, 3962–72.
(22) Werst, M. M.; Davoust, C. E.; Hoffman, B. M. *J. Am. Chem. Soc.* **1990**, *113*, 1533–8.
(23) Carrington, A.; McLachlan, A. D. *Introduction to Magnetic Resonance*; Harper and Row: New York, 1967.
(24) Hoffman, B. M.; Roberts, J. E.; Swanson, M.; Speck, S. H.; Margoliash, E. *Proc. Natl. Acad. Sci. U.S.A.* **1980**, *77*, 1452–6.
(25) Werst, M. M.; Fee, J. A.; Hoffman, B. M. Unpublished results.

It is possible that Ni binds H^- or H_2, but that XAS is not sufficiently sensitive to detect the interaction. This would require the interaction between Ni and H_2 (or H^-) to not appreciably perturb the electron density at the Ni site or the Ni site structure. Further, it is difficult to account for the weak coupling observed in the ENDOR if the H^- is a Ni ligand. It is also possible that the hydrogenic species is not a Ni ligand. This latter possibility cannot be ruled out on the basis of current EPR and ENDOR data, and it is consistent with the XAS analysis. Active enzyme exposed to ^{13}CO reveals a strong ^{13}C hyperfine interaction that has been interpreted in terms of CO bound to the Ni center via a metal orbital containing unpaired spin density.[11] The fact that ^{13}CO bound to the enzyme reveals strong ^{13}C hyperfine interaction ($A_{x,y,z}$ = 85.3, 88.0, 90.3 MHz)[11] and that paramagnetic Ni hydrides[26,27] also have large couplings to the H^- ligand, but H_2 (or H^-) shows a much weaker coupling (A(H2) ~ 20 MHz) in Ni-C, provides an argument against a strong bond to H^- or H_2 at the same Ni site. Other possible binding sites include Fe,S clusters, which are present in all H_2ases and are the likely binding sites for H_2 in Fe-only H_2ases,[1] and sulfide ligands. The possible presence of a Ni,Fe,S cluster in the active site in Fe,Ni H_2ases, as suggested by EPR[7,9,13] and EXAFS studies,[21] could give rise to a mechanism by which weak coupling between the hydrogenic proton(s) bound to the Fe,S cluster and the Ni center could occur. Another possibility is that activation of H_2 involves interaction with a sulfide ligand of Ni and/or an Fe,S cluster. It is not possible from XAS analysis to differentiate between thiolate and sulfide ligands, thus the possibility of a Ni sulfide ligand exists. Further, heterolytic cleavage of H_2 (the reaction catalyzed by H_2ase[28]) involving a bridging sulfide has been demonstrated to occur in one model system.[29]

Conclusions

From the studies presented here, several points regarding hydride or dihydrogen binding to hydrogenase can be made:

1. The conversion of Ni-C to Ni-L involves the photolytic cleavage of a hydrogenic species derived from H_2.

2. Annealing the sample at 200 K re-establishes the interaction between the binding site and the hydrogenic proton(s).

3. XAS studies reveal no significant structural difference in the Ni sites between Ni-C and Ni-L. This opens the possibility that the hydrogenic species seen by ENDOR spectroscopy is not a Ni–H or Ni–H_2 complex.

Experimental Section

Sample Preparation. Cultures of *Thiocapsa roseopersicina* BBS were kind gifts from Dr. I. N. Gogotov, Institute of Soil Sciences, Puchino, Russia, and from Dr. Kornel Kovacs, Biological Research Institute, Hungarian Academy of Sciences, Szeged, Hungary. The bacteria were grown in a modified Pfennig's media illuminated with incandescent light at room temperature. The cultures were harvested in the late logarithmic phase of growth and the cell paste was stored at −20 °C. In 300-g batches, the cell paste was converted to an acetone powder as previously described.[30] The hydrogenase enzyme was purified from the acetone powder using a minor modification of a published procedure.[30] Final purification of the H_2ase was achieved by preparative gel electrophoresis. Ar and H_2 gases used in manipulating the redox state of the enzyme were of the highest grade available and purified by passage through Oxisorb cartridges (MG Industries).

The sample used to obtain ENDOR spectra of H_2ase in H_2O was prepared by concentrating 6 mg of the H_2ase enzyme in Tris-HCl (pH 7.5) to 120 μL using a hollow fiber bundle concentrator (Bio-Molecular Dynamics). The sample was evaporated to a final volume of 40 μL under pure H_2. In this case, the sample was prepared in an ENDOR tube, which allowed for a slower diffusion of the gas through the sample. The progress of the formation of form C could be monitored by following the partial bleaching of the color of enzyme as it was converted from the more oxidized forms of the enzyme to form C. Completion of this process took about 6 h at room temperature. The sample was then incubated under Ar for 2 h in order to increase the signal to form C (e.g. to reoxidize it from the more reduced form of the enzyme).

The sample used to obtain ENDOR spectra of H_2ase in D_2O was prepared by dissolving 9 mg of the H_2ase enzyme in Tris-DCl (pD 7.5) by first concentrating the sample to 120 μL as before and then diluting it to 4 mL with the deuterated buffer. This exchange was repeated ten times, and the sample from the final concentration was transferred into an ENDOR tube. The sample was then evaporated to a final volume of 40 μL under pure H_2. The conversion to form C took about 8 h under H_2 at room temperature, with further incubation under Ar for 3 h in order to maximize the EPR signal of form C. This sample was also used for XAS measurements (form C) after the ENDOR experiment.

The light-exposed form, Ni-L, was made by irradiating the form C sample with an intense light source for ca. 1 h while the samples were immersed in liquid N_2. The EPR signal was monitored during irradiation in order to ascertain when maximal conversion to the photoproduct had been achieved. The integration of the EPR signal of the irradiated sample (Ni-L) was 90–92% of the integration of the corresponding form C signal (Ni-C).

EPR. EPR experiments for the purpose of characterizing the photochemistry of form C and for monitoring redox poise and sample integrity were performed at 77 K at the University of Massachusetts using an IBM ER300 spectrometer. Temperature-dependent EPR studies designed to examine the annealing process were performed at Amherst College on a Bruker ER220D-SRC equipped with an Oxford cryostat. The conversion of Ni-C to Ni-L for the initial spectrum integrated to 92% of the Ni-C signal before illumination. The composition of the spectra obtained after equilibration at temperatures in the range of 4.2–250 K was determined by fitting the spectrum using the initial (Ni-L) and final (Ni-C) spectra. Fits of EPR data were performed using the program SPSERV.

ENDOR. The ENDOR spectra were obtained at 2 K at Northwestern University on a locally constructed spectrometer that is described elsewhere.[22] The cw ENDOR signals were observed as a decrease in the 100 kHz modulated, dispersion mode EPR signal. All cw ENDOR patterns were observed with both increasing and decreasing frequency sweeps; parameters reported are the average of these measurements. The experiments were performed on samples of protein dissolved in either ^1H_2O or ^2H_2O (D_2O). The EPR and ENDOR spectra taken after illuminating the sample with a xenon lamp are labeled "Ni-L" and compared to corresponding spectra of the "dark" Ni-C sample. A set of magnetically equivalent protonic species, H = ^1H, ^2H, gives a pair of ENDOR transitions ($\nu_\pm$) centered about the Larmor frequency,[31,32]

$$\nu = \left|\nu(\mathrm{H}) \pm \frac{A(\mathrm{H})}{2}\right| \qquad (1)$$

$\nu_H = (g_H\beta_n/\beta_e)(\nu(M)/g_{obs})$, which varies with the EPR spectrometer frequency. For ^2H nuclei (I = 1) the additional splitting of the ENDOR lines due to quadrupolar interaction is predicted, but such a splitting was not observed. For a fixed g_{obs} the center of the proton resonance pattern shifts in proportion to the microwave frequency ν(M). An increase in ν(M) from 9 GHz (X-band) to 35 GHz (Q-band) increases ν_H (at g ~ 2) from ~14 MHz to ~53 MHz, which eliminates spectral overlap of proton signals with those of ^{14}N (or other nuclei). The Larmor frequencies of ^1H and ^2H obey the relation

$$\frac{\nu(^1\mathrm{H})}{\nu(^2\mathrm{H})} = \frac{A(^1\mathrm{H})}{A(^2\mathrm{H})} = 6.51 \qquad (2)$$

Such a difference in Larmor frequencies separates completely proton and deuterium signals. The samples employed in this study were frozen solutions. The analysis of spectra from such samples have been previously described.[33–36]

(26) Symons, M. C. R.; Aly, M. M.; West, D. X. *Chem. Commun.* **1979**, 51–2.
(27) Morton, J. R.; Preston, K. F. *J. Chem. Phys.* **1894**, *81*, 5775–78.
(28) Krasna, A. I. *Enzyme Microb. Tech.* **1979**, *1*, 165–72.
(29) Laurie, J. C. V.; Duncan, L.; Haltiwagner, R. C.; Weberg, R. T.; DuBois, M. R. *J. Am. Chem. Soc.* **1986**, *108*, 6234–41.
(30) Kovacs, K. L.; Tigyi, G.; Alfonz, H. *Prep. Biochem.* **1985**, *15*, 321–34.
(31) Abragam, A.; Bleaney, B. *Electron Paramagnetic Resonance of Transition Ions*; Clarendon Press: Oxford, 1970.
(32) Atherton, N. M. *Electron Spin Resonance*; John Wiley: New York, 1973.
(33) Rist, G. H.; Hyde, J. S. *J. Chem. Phys.* **1970**, *52*, 4633–43.
(34) Hoffman, B. M.; Martinsen, J.; Venters, R. A. *J. Magn. Reson.* **1984**, *59*, 110–23.
(35) Hoffman, B. M.; Martinsen, J.; Venters, R. A. *J. Magn. Reson.* **1985**, *62*, 537–42.

XAS. Ni K-edge XAS data were collected at the National Synchrotron Light Source at Brookhaven National Laboratories on beamline X9A. The data were collected from 8.1 to 9.2 keV, under dedicated conditions (2.53 GeV, 60–120 mA) using a Si[111] crystal monochromator. This arrangement provided a theoretical resolution of ca. 1 eV at 8.3 keV for a 1 mm hutch slit height. However, edge energy calibrations were reproducible to within ±0.2 eV. Harmonic rejection was achieved by the use of a Ni focusing mirror in the beam path set at an angle of 5 mrad. The energy scale of the XAS spectra was calibrated to the first inflection point in the nickel foil spectrum (8331.6 eV) as previously described.[15] Incident radiation (I_0) was measured using an N_2 filled ionization detector, while the transmission data were measured using an Ar filled detector. Fluorescent data were collected on the enzyme samples contained in polycarbonate sample holders, which allowed XAS and EPR spectra to be measured without thawing the samples, by using a 13-element Ge detector (Canberra). For XAS measurements, the sample holders were inserted into slotted Al holders. The spectra were measured at 25 K using a liquid He displex unit.

The integrity of the XAS samples following exposure to synchrotron radiation was determined by monitoring the edge spectra as a function of exposure time and by comparing EPR spectra taken on the samples before and after exposure. The edges were not affected by exposure time, indicating that the Ni center was not oxidized or reduced in the beam. The EPR spectral comparisons revealed no changes in the enzyme signal or signal intensity after exposure to synchrotron radiation for either form C or its photoproduct. The amount of protein in the samples was determined after measuring the EXAFS spectra and final EPR spectrum, by diluting the whole sample and measuring the absorbance at 220 nm (ϵ = 89 500 cm^{-1} M^{-1}) and 280 nm (ϵ = 10 600 cm^{-1} M^{-1}).[15]

The XAS spectra were summed, background corrected, and normalized by standard procedures.[16,37] To aid in the comparison of spectra taken on different samples, the signal-to-noise ratio of a given set of data was calculated. The edge jump height was taken as a measure of the signal. An estimate of the noise was taken by fitting a second-order curve to a section of the XAS data where all of the waves had damped out (approximately 8900 eV), and the value of σ was taken as a measure of the noise in a summed spectrum. For purposes of comparison, "the edge energy" is taken as the energy at a normalized absorbance of 0.5. The areas under the peaks assigned to 1s → 3d transitions were determined by subtracting a fit to the edge (arctan or Fermi functions) from the pre-edge region and integrating the difference spectrum. The EXAFS data were corrected for detector efficiencies, absorbance by air and cryostat windows, and the variation with energy of the sample X-ray penetration depth.[16] Least-squares fits of the EXAFS data over the k range of 2–12.5 $Å^{-1}$ were performed as previously described.[21] Fourier-filtered spectra were generated using a backtransform window of 1.1–2.7 Å (without phase shift correction). Empirical parameters used in generating the fits (amplitude reduction factors, Debye–Waller factors, E_0) were obtained from transmission data previously collected from model compounds, $[Ni(Im)_6](BF_4)$ and $(Et_4N)_2[Ni(p\text{-}SC_6H_4Cl)_4]$.[21]

Acknowledgment. Funding for this work was provided by a grant to M.J.M. from the NIH (GM 38829) and grants to B.M.H. from the NSF (DBM 8907559) and NIH (HL 13531). We thank the Biostructures PRT, which is supported by a grant from the NIH (RR 01633), for beam-time allocations and access to equipment. We are also indebted to Prof. Robert Scarrow for providing a copy of his EXAFS analysis package, SEXAFS, to Prof. David Dooley for the use of his EPR spectrometer, and to Dr. Syed Khalid, Dr. Petra Turowski, and Manju Sharma for experimental support. We also thank Prof. Simon Albracht for information regarding the redox properties of *Chromatium vinosum* hydrogenase prior to publication and for many helpful comments.

Supplementary Material Available: Tables of fits of EXAFS data (12 pages). Ordering information is given on any current masthead page.

(36) Hoffman, B. M.; Gurbiel, R. J.; Werst, M. M.; Sivaraja, M. In *Advanced EPR. Applications in Biology and Biochemistry*; Hoff, A. J., Ed.; Elsevier, Amsterdam, 1989; pp 541–91.

(37) Scott, R. A. *Meth. Enzymol.* **1985**, *117*, 414–59.